Electron-electron correlations in diamond: An x-ray-scattering experiment

C. Petrillo and F. Sacchetti
Dipartimento di Fisica, Universitá di Perugia, Via A. Pascoli, I-06100 Perugia, Italy
and Istituto Nazionale di Fisica della Materia, Unitá di Perugia, Perugia, Italy
(Received 19 August 1994)

The inelastic-scattering cross section integrated over the energy has been measured in diamond from an x-ray-scattering experiment. The static structure factor and the exchange and correlation energy of the electrons in diamond have been determined. From the static structure factor, the electron-electron pair correlation function has been deduced. Comparisons have been carried out with both recent quantum Monte Carlo calculations in diamond and calculations for the jellium model.

I. INTRODUCTION

The quantitative understanding of the electron correlations in real many-electron systems still represents a challenge in condensed-matter physics. A correct description of the ground state, as well as the excited states, cannot leave the role of the electron correlations out of consideration. Many properties of real solids, among which the cohesive energy, the bulk modulus, and the size of the band gap in semiconductors, are known to be inadequately accounted for by one-electron-approximation treatments. Moreover, settling in of a magnetic phase, even in the simplest system such as a transition metal, depends on a competition between intra-atomic exchange interactions and interatomic electron correlations. Therefore, accurate *ab initio* calculations in solids must include, as a fundamental contribution, a treatment of the electron correlations. This problem is now relatively well understood in a model system like the homogeneous electron gas[1,2] and not only in the two limiting cases of very high and very low densities.[3,4] Indeed Fermi Monte Carlo simulations allowed for a description of the electron gas also at intermediate values of r_s, that is in the metallic region.[5]

A direct measure of the correlations between pairs of electrons is offered by the two-body correlation function. Since the Coulomb interaction, which embodies the whole of the electron-electron interactions, is a purely two-body one, the behavior of the electron system is fully described by the two-body correlation function. In principle, with the knowledge of this function the ground-state potential energy of the interacting electron system, and hence the ground-state energy via the virial theorem at zero external pressure,[6] can be calculated.[7] The relationship between the two-body correlation function and the ground-state energy, which is trivial for the model system of the homogeneous electron gas,[7] can be generalized and applied to electrons in real solids,[8] properly taking into account the external periodic potential of nuclei. Finally, the basic role of the two-body correlation function in fully describing the interacting electron system, has been enlightened by the density-functional formalism.[9] Generalization of the Hellmann-Feynman theorem[10,11] within the density-functional theory, shows that[9] the exact exchange-correlation energy of the interacting electron system with density $n(r)$ and Coulomb interaction λV_{ee} is given by an integration of the two-body correlation function over the coupling constant λ. Of course the knowledge of the two-body correlation function as a continuous function of the coupling constant λ would require the solution of the many-electron problem, which is currently very difficult. Nevertheless, extensive calculations of this function in several real solids should be afforded in order to get a deeper understanding of the Coulomb and Fermi hole surrounding each electron and describing the effect of the electron-electron interaction. The computational complexity of the problem has however limited the calculations to very few solid systems.[12–14]

On the other hand, the experimental determination of electron-electron correlations has been carried out in few and light elements like solid Be,[15] Al,[16] and Si,[17] and only in the case of Be (Ref. 15) a rather extended investigation of the two-electron correlation function is available. This circumstance can be explained considering that the only efficient way to measure the pair correlation function is through a properly designed x-ray-diffraction experiment. By this technique the static structure factor, which is the Fourier transform of the pair correlation function, can be measured. Since the most important contribution to the pair-correlation function comes from the valence or conduction electrons, the core electron contribution representing a sort of less interesting background, experiments have been confined to light elements where the number of core electrons is relatively small as compared with the total number of electrons. An additional constraint to the experimental study of heavy elements is represented by the considerable increase of the photoabsorption cross section with increasing the atomic number. Furthermore, the contribution to the scattering due to the thermal nuclear motion, which has to be subtracted, represents a limitation and experiments can be carried out in systems characterized by a high Debye temperature.

Recently, theoretical calculations of the ground-state wave function, from which the pair correlation function can be deduced, have been performed in diamond[12,14] and hydrogen,[13] based on the quantum Monte Carlo ap-

0163-1829/95/51(8)/4755(8)/$06.00

proach. For both these systems the experimental information on electron correlations is to our knowledge, still lacking. In order to provide the experimental data against which these calculations can be checked, we carried out the measurement of the electron-electron correlations in diamond by an x-ray-scattering technique that yields a direct determination of the static structure factor. Diamond, as Be, is particularly suited for this sort of investigation because of its simple structure and high symmetry. Moreover, as in Be, the number of valence electrons is large as compared with the total number of electrons. On the contrary, diamond represents a prototype of a covalent insulating solid, where the valence electrons have a rather anisotropic distribution with a high electron density along the tetrahedral bonds. This feature makes the comparison with Be interesting, where the valence electrons are almost homogeneous electron gas at the appropriate density. Finally, diamond is relatively transparent to medium energy photons (10–20 keV) and its very low thermal motion, reflected in the high Debye temperature, makes the corrections for thermal diffuse scattering (TDS) fairly small.

In the following sections the basic relationship between the x-ray scattering cross section and the static structure factor in a single crystal is briefly outlined and discussed in close connection with the experimental procedure. Finally, results are presented and discussed.

II. EXPERIMENTAL DETERMINATION OF THE STATIC STRUCTURE FACTOR

The relationship between the x-ray cross section and the two-body correlation function has been discussed in detail in Ref. 15 and we will closely follow the formalism there developed. The x-ray differential scattering cross section in a light element like diamond, for incoming photon energies much greater than the typical excitation energy in the system (that is greater than the energy of the K absorption edge) and for momentum transfers $\mathbf{Q}$ different from all the reciprocal-lattice vectors (that is when the orientation of the crystal is such that no Bragg diffraction occurs), is given by[15]

$$\frac{d\sigma}{d\Omega} \simeq r_0^2 N \left[\frac{k}{k_0} d_f (\bar{e}_0 \cdot \bar{e})^2 S(\mathbf{Q}) + S_{\mathrm{TDS}}(\mathbf{Q}) \right] , \tag{1}$$

where r_0 is the classical electron radius, $\mathbf{k}_0$ and $\mathbf{k}$ are the incoming and outgoing photon wave vectors, $\bar{e}_0$ and $\bar{e}$ are the corresponding polarization unit vectors, N is the number of atoms within the sample, $S_{\mathrm{TDS}}(\mathbf{Q})$ is the TDS structure factor, and $S(\mathbf{Q})$ is the static structure factor one is looking for. d_f is a kinematic correction related to the number of final states[18] and given by

$$d_f = \hbar c \left[\frac{\partial k}{\partial E_f} \right]_{2\vartheta = \mathrm{const}} , \tag{2}$$

where E_f is the total energy of the final state and the derivative has to be performed at constant scattering angle 2ϑ. A reasonable approximation to d_f is offered, as in the case of Be,[15] by the following relationship:

$$d_f \simeq \frac{k}{k_0} , \tag{3}$$

with k/k_0 given by the result for the free-electron case, namely the Compton formula. It should be remarked that such an approximation is appropriate for light elements only since, in such a case, the electron binding energy is negligible in comparison with that of the incoming photon. The validity of Eq. (3) relies also on the limiting behavior $d_f \rightarrow 1$, with decreasing the scattering angle. The factor d_f can differ appreciably from 1 at high scattering angles only, that is, in a region where the cross section is dominated by the single-particle regime or by the Compton scattering. For instance, employing the Compton formula in Eq. (3), results in $d_f = 0.959$ at $\hbar c k_0 = 22$keV and $2\vartheta = 90°$. Therefore, d_f is always very close to 1 and hence the proposed approximation can be considered as a meaningful one.

It should be remembered that the validity of Eq. (1) relies on the approximations[15] that an efficient integration over all the inelastic-scattering events is performed and that the final photon energy is confined within a relatively small range around the average value $\hbar c k$. This average final energy, according to the above discussion on d_f, can be assumed equal to that derived by the Compton formula. Therefore, an experiment devoted to the measurement of $S(\mathbf{Q})$ should be performed employing an incoming photon energy as high as possible and a detector system having a wide and uniform acceptance band for the scattered photons.

In order to measure the cross section described by Eq. (1), we performed an x-ray-diffraction experiment employing Ag $K\alpha$ radiation, whose energy is high enough as compared with the K absorption edge of carbon. By this choice of wavelength, a still acceptable momentum transfer resolution could be obtained. An intense and clean incoming beam was produced using a pyrolitic graphite flat monochromator, which avoided the contamination of the beam from K_β radiation. The take-off angle at the monochromator was rather small and, as a consequence, the incoming beam was unpolarized, as ascertained by a direct measurement of the linear polarization.[15] Since the measurement of $S(\mathbf{Q})$ implies the integration over the energy of the scattered photons, the scattered intensity was collected employing a broad band device. A 0.2 cm thick NaI:Tl scintillator detector followed by a pulse-height analyzer was used for photon collection. The energy resolution we obtained was about 5 keV. The energy bandwidth of the system was set from 10 to 35 keV. In such a way the contribution from half-wavelength contamination, present in the incoming beam, was almost completely rejected, while the uniformity of the counter efficiency was expected to be better than 0.1%. The incoming beam was vertically collimated by a tungsten Soller slit having 3° full width at half maximum (FWHM), while it was horizontally defined by a slit matched to the mosaic spread of the monochromator, so that the beam had 0.6° FWHM. A tungsten Soller slit, 1 cm wide, was used before the detector. The Soller slit allowed for an optical configuration with a rather sharp angular resolution and, at the same time, with all the

bathed portions of the sample to be seen with the same weight by the detector. The incoming beam profile was experimentally determined by measuring the intensity of the (111) reflection from a copper wire having a 0.008-cm diameter. The FWHM of the beam profile turned out to be 0.12 cm with a little asymmetry.

The sample employed in the present experiment was a natural diamond of grade A supplied by Drukker International. It was disk shaped, 0.3-cm diameter, and 0.05-cm thickness, with the extended face parallel to the (110) crystallographic plane. Six kinds of coupled $(\omega-2\vartheta)$ scans were performed on the sample after initial missetting of the crystal $+5°$ and $-5°$ off the three principal crystallographic directions, namely, [100], [110], and [111]. It should be noted that the quasielastic scans corresponding to positive and negative missettings collected along each of the three maximum symmetry directions, with the present crystal in symmetric transmission, should be equal, that is they should yield the same static structure factor $S(\mathbf{Q})$ and the same TDS structure factor $S_{\mathrm{TDS}}(\mathbf{Q})$. However, some of the corrections to be applied to the raw data depend on the angle and they are not the same for positive and negative missettings. With the proposed scan configuration it is possible to avoid the extremely intense Bragg-peak contributions and to check the validity of the various angle-dependent corrections as well. In Fig. 1, the scan geometry superimposed to the reciprocal lattice is shown.

The raw data were corrected for background, transmission, and multiple scattering employing a Monte Carlo program similar to that successfully applied to neutron-diffraction data reduction.[19] Effects due to the finite size of both the beam and the sample and effects due to partial polarization of the beams propagating inside the crystal were also taken into account by inserting the experimental shape of the incoming beam and the appropriate scalar product of the polarization vectors in the Monte Carlo program. The program also requires as input data the total linear attenuation coefficient, set equal to 11.4 cm^{-1}, the static structure factor and the TDS structure factor. Since the true structure factor is unknown and it should result from the present experimental investigation, we employed as reference input the structure factor of the carbon free atom. Of course, x-ray-scattering measurements of this function do not exist as the sample would be a low-density carbon atom gas. The static structure factor of the atom is then supplied by accurate first-principles approach, one of the most common being the Hartree-Fock one, which, however, accounts for the Pauli repulsion only. Another theoretical treatment where effects beyond Hartree-Fock, i.e., correlation effects, are included is that known as configuration interaction (CI), based on the use of an improved many-particle function. However, only systems with relatively few electrons can be calculated with high accuracy because of the large increase in the number of configurations required with increasing the atomic number. In the specific case of diamond, both the Hartree-Fock[20–22] and the CI (Ref. 20) calculations of the atomic static structure factor are available. In order to minimize the error introduced by the use of calculated quantities,

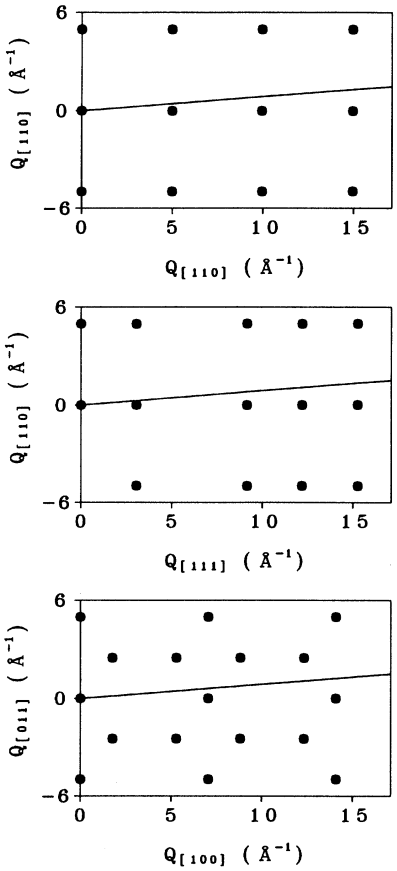

FIG. 1. Reciprocal-lattice sections showing the line followed by the $(\omega-2\vartheta)$ scans for both $+5°$ and $-5°$ missetting of the crystal out of the three crystallographic directions [110] (upper panel), [111] (central panel), and [100] (lower panel).

we preferred to make use of the more accurate CI calculation.[20] The TDS structure factor was calculated as the sum of one-phonon and multiphonon terms, the one-phonon contribution being calculated in an harmonic approximation using the experimental phonon dispersion relations of diamond as fitted in Ref. 23, and the multiphonon term being evaluated by means of the static approximation[24] and using the phonon density of states still from Ref. 23. Finally, the calculation of the TDS structure factor requires, as input, the scattering factor of the crystal. Since this function does not differ substantially from that of the free atom (the average ratio being $\simeq 1.01$ over the $\sin\vartheta/\lambda$ range corresponding to the first 9 Bragg reflections in the crystal), the scattering factor of the free carbon atom, as calculated in Ref. 21, was employed. This computational procedure is expected to be fairly good considering that the Debye temperature of diamond is much higher than the room temperature and hence the TDS cross section is dominated by the one-phonon contribution. As an example, Fig. 2(a) shows the calculated one-phonon and multiphonon TDS structure factors along the [100] crystallographic direction. The total TDS structure factor amounts to $\simeq 0.2-0.4$ and this value has

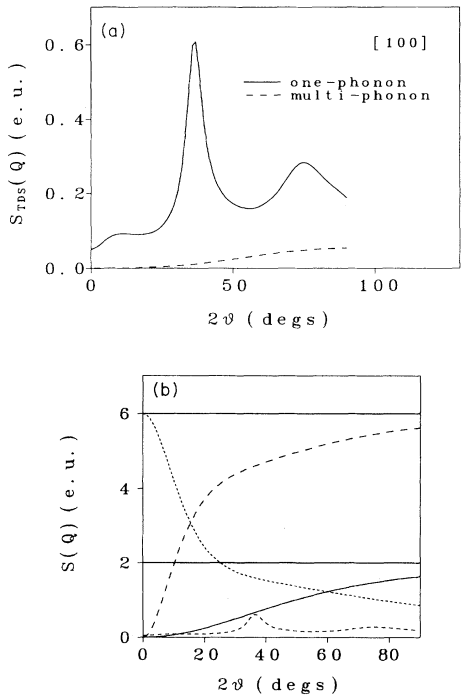

FIG. 2. (a) The TDS static structure factor versus the scattering angle calculated along the [100] direction. Both the multiphonon (dashed line) and the one-phonon (full line) contributions are shown (see text). (b) Different contributions to the measured intensity. Free-atom structure factor (Ref. 20) (dashed line), TDS total structure factor (short-dashed line), core electron structure factor (Ref. 25) (full line), free-atom scattering factor (Ref. 21) (dotted line). The horizontal full lines are reference levels.

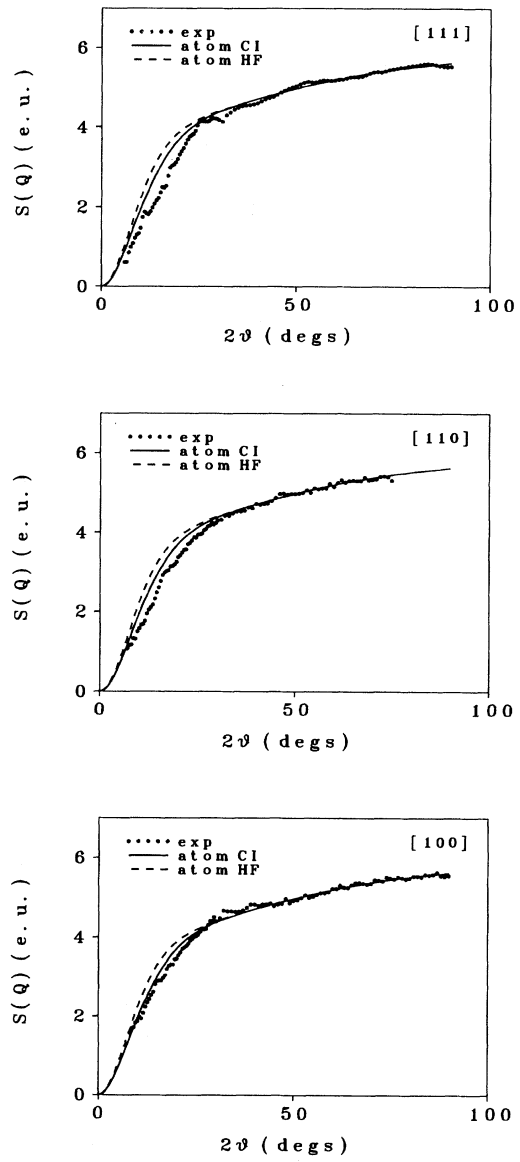

FIG. 3. Measured static structure factor (dots) versus the scattering angle and for [111] (upper panel), [110] (central panel), and [100] (lower panel) directions. The free-atom static structure factor is also shown: CI calculation (Ref. 20) (full line) and Hartree-Fock calculation (Refs. 20–22) (dashed line).

to be compared with 6, i.e., the limiting value of the static structure factor at high-momentum transfer. In Fig. 2(b) the various contributions to the measured intensity are shown, namely, the free atom[20] and the TDS structure factors, the free-atom scattering factor[21] and, for comparison purposes, the core structure factor[25] that will be discussed in the following. In such a figure the multiple-scattering contribution is not reported since it is almost flat and of the order of 0.2%. The accuracy of the whole correction procedure was checked by comparing the various scans collected for both positive and negative missettings. The agreement between the two sets of data was in all cases better than 2%. The so-corrected data were then put on an absolute scale by normalizing the experimental cross section to the free-atom theoretical one at high-momentum transfer, where solid-state effects are expected to be very small and it holds,

$$\lim_{Q\to\infty} S(Q)=Z \ , \tag{4}$$

Z being the atomic number. The normalized data, after subtraction of the TDS and multiple-scattering contributions, are shown in Fig. 3. Considering the sharp peaks exhibited by the TDS cross section and the rather smooth behavior of the curves shown in Fig. 3, one can be quite confident that the various corrections were treated accurately. In this figure, the experimental data are also superimposed to the Hartree-Fock[20–22] and CI (Ref. 20) structure factors calculated for the free atom. Such a comparison enhances the inadequacy of the Hartree-Fock calculation, which produces a systematically higher atomic structure factor in the region of low exchanged momentum and hence an expected value of the cohesive energy too high, this latter being roughly proportional to the difference between the experimental and the atomic structure factors.

III. DISCUSSION

The measured structure factors embody the electron-electron correlations of all the electrons in diamond. However solid-state effects are expected to be more pronounced for valence electrons. The distinction between core and valence electrons is somewhat arbitrary but, in view of the large energy separation between K and L excitation energies, a meaningful separation can be tempted. Therefore, the static structure factor can be written as the sum,

$$S(\mathbf{Q})=S_{\rm val}(\mathbf{Q})+S_{\rm core}(Q)\ . \tag{5}$$

In Eq. (5) the core-orthogonalization contribution is neglected considering that it is, in any case, fairly small.[15,20] Through Eq. (5), $S_{\rm val}(\mathbf{Q})$ can be obtained along the three maximum symmetry directions, provided an adequate representation of $S_{\rm core}(Q)$. In particular, we assumed that core electrons were well described by the configuration-interaction wave functions calculated for the C^{4+} ion in Ref. 25. $S_{\rm core}(Q)$ thus deduced is shown in Fig. 2(b), while the resulting valence-electron static structure factor is shown in Fig. 4. The most striking feature of $S_{\rm val}(\mathbf{Q})$ is its anisotropy as revealed in Fig. 4 by the well-defined dependence on the direction of the momentum transfer. This dependence agrees with the guess that more charge is accumulated along the [111] direction, which is parallel to the first-nearest-neighbor bonds. Moreover, $S_{\rm val}(\mathbf{Q})$ extends towards high Q according to the fact that the Fermi momentum is proportional to the cube root of the density in the homogeneous electron gas. This behavior is also in agreement with that exhibited by the pair correlation function calculated by the quantum Monte Carlo method in Refs. 12 and 14. Indeed the calculated Fermi and Coulomb holes were found more contracted along the [111] direction, especially when the first electron was at the bond center.[12,14]

In order to understand the effects of the electron correlations in diamond, in view of the anisotropy exhibited by the valence structure factor, the relationships linking $S(\mathbf{Q})$ to the pair correlation function $g(\mathbf{r},\mathbf{r}')$ and to the expectation value of the exchange-correlation energy should be exploited. According to Refs. 8 and 15, one can write

$$S(\mathbf{Q})=Z+\int d\mathbf{r}\,d\mathbf{r}'n(\mathbf{r}')n(\mathbf{r}'+\mathbf{r})\times[g(\mathbf{r}',\mathbf{r}'+\mathbf{r})-1]e^{-i\mathbf{Q}\cdot\mathbf{r}}\ , \tag{6}$$

and

$$V_{\rm xc}=\frac{e^2}{2}\int d\mathbf{r}\int d\mathbf{r}'\frac{1}{|\mathbf{r}-\mathbf{r}'|}\times[\langle 0|\hat{\rho}^{+}(\mathbf{r})\hat{\rho}(\mathbf{r}')|0\rangle-n(\mathbf{r})n(\mathbf{r}')]=\frac{e^2}{4\pi^2}\int d\mathbf{Q}\frac{S(\mathbf{Q})-Z}{Q^2}\ , \tag{7}$$

where $n(\mathbf{r})$ is the electronic ground-state number density and $\hat{\rho}(\mathbf{r})$ is the electronic number density operator. Equation (6) shows that in an inhomogeneous system, where the pair-correlation function depends on the individual electron coordinates and not simply from their difference and the density is a varying function of the position, it is not possible to derive the pair correlation function from a scattering experiment. Nonetheless a position averaged correlation function, which is a measure of the probability of finding two electrons at the distance $\mathbf{r}$ independently of their individual positions relative to the crystal, can be defined. One has

$$\bar{g}(\mathbf{r})=\frac{1}{(2\pi)^3\bar{n}Z}\int d\mathbf{Q}[S(\mathbf{Q})-Z]e^{i\mathbf{Q}\cdot\mathbf{r}}=\frac{1}{\bar{n}}\int d\mathbf{r}'n(\mathbf{r}')n(\mathbf{r}'+\mathbf{r})[g(\mathbf{r}',\mathbf{r}'+\mathbf{r})-1]\ , \tag{8}$$

where $\bar{g}(\mathbf{r})$ is the averaged pair-correlation function and $\bar{n}$ is the average number density.

The use of Eqs. (7) and (8) still requires the knowledge of $S(\mathbf{Q})$ everywhere in the reciprocal space, whereas the measurement of $S(\mathbf{Q})$ is limited to few high-symmetry directions. A practical use of these equations would resort to some appropriate approximation for the angular dependence of $S(\mathbf{Q})$, once such dependence is known for a finite set of directions as it is in the present investigation. The simplest way to proceed is substituting $S(\mathbf{Q})$ by an appropriate spherical average, that is

$$S_{\rm av}(Q)=\frac{8S(\mathbf{Q}_1)+6S(\mathbf{Q}_2)+12S(\mathbf{Q}_3)}{26}\ , \tag{9}$$

where $\mathbf{Q}_1$, $\mathbf{Q}_2$, and $\mathbf{Q}_3$ refer to the three maximum-symmetry directions, namely [111], [100], and [110], respectively, and the weights are given by the multiplicity. Alternatively, general symmetry arguments can be applied in order to provide an interpolation formula between the data experimentally collected.[26] For the present purposes, we preferred to analyze the data by means of the approximate average of Eq. (9).

The value of the exchange and correlation potential obtained by integrating Eq. (7) with $S_{\rm av}(Q)$ given by Eq. (9) is reported in Table I. We note that the integration over the momentum transfer Q, virtually extending from 0 to ∞ cannot be carried out by simply using the experimental data that are collected over a finite Q range. This difficulty was overcome by exploiting either the close

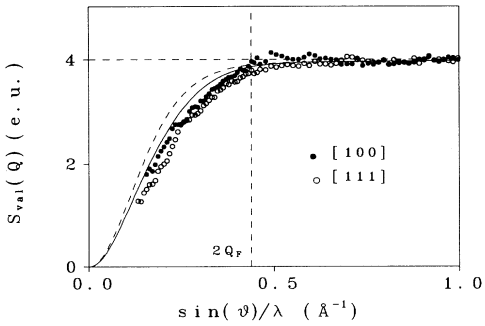

FIG. 4. Valence-electron static structure factor. Experimental data collected along [100] (dots) and [111] (circles) directions, free-atom CI calculation (Ref. 20) (full line), and Hartree-Fock (Refs. 20–22) calculation (dashed line).

TABLE I. Exchange and correlation (V_{xc}), electrostatic Hartree ($V_{Hartree}$), and total (V_{tot}) interaction potential. Results from the present experiment are compared with those obtained for the free atom and with the quantum Monte Carlo calculated values in diamond (Refs. 12 and 14). The cohesive energy (E_{coh}) is also quoted.

	V_{xc} (Ry)	$V_{Hartree}$ (Ry)	V_{tot} (Ry)	E_{coh} (Ry)
Present experiment	−11.91	−140.09	−152.00	0.44
C atom	−11.27	−139.85	−151.12	
Theory (Ref. 14)			−152.21	0.55

resemblance of $S_{av}(Q)$ with the atomic structure factor[20] at momentum transfers $Q > 6$ Å^{-1} or the limiting parabolic behavior of $S(Q)$, when $Q \to 0$ as dictated by general arguments.[10] Therefore the number quoted in Table I refers to the integration over the full Q range. For sake of comparison, the purely electrostatic Hartree term, $V_{Hartree}$ was calculated for the crystal following the formalism of Ref. 8 and making use of measured scattering functions as quoted in Ref. 27. This term is reported in Table I, together with the total interaction potential V_{tot}.

A theoretical estimate of V_{tot} can be obtained from the quantum Monte Carlo calculation[12,14] on diamond. From Table I, a difference of $\simeq 0.2$ Ry between the theoretical and the experimental values of V_{tot} is observed. The value of this difference represents a very small percentage of the total interaction potential and it could be due to inaccuracies in both the numerical simulation and the experimental estimate of the large Hartree term for which the measured data from Ref. 27 were used.

In the case of the free atom, the interaction potential can be evaluated following the same scattering function approach as for the solid and making use of the appropriate static structure factor. The relevant relationships are reported in Refs. 8 and 15. Results of the calculation performed using the carbon free-atom scattering factor, as calculated in Ref. 21, are reported in Table I. Taking the difference of the total interaction potential between the solid, and the atom yields the double of the cohesive energy. The value 0.44 Ry for the cohesive energy as deduced from the scattering approach applied to both the solid and the atom is compared in Table I with the experimental value 0.54 Ry, deduced from thermodynamic measurements, which is in very good agreement with the Monte Carlo calculation (0.55 Ry).[14]

From the present data, a spherical pair correlation function $\bar{g}(r)$ might be calculated by using the experimental average structure factor. In order to avoid the numerical difficulties implied by the direct Fourier transform of $S_{av}(Q)$, we followed a procedure similar to that applied in the case of Be.[15] In particular, a model pair correlation function containing four free parameters and quite similar to that introduced in Refs. 28 and 29 was assumed. Such a function must obey a number of constraints[28,29] that provide explicit relationships among the free parameters, in fact reducing the number of effective

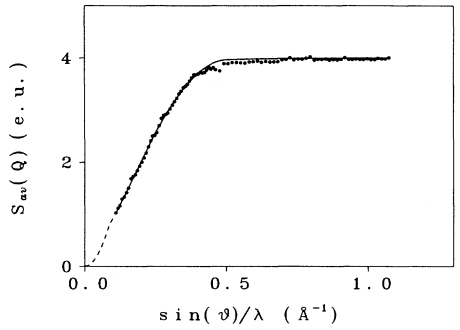

FIG. 5. Experimental average static structure factor [see Eq. (9)]. The full line is the best-fit result for the model structure factor (see text). The initial dashed portion of the curve is a guide to the eye.

parameters to two. The values of the two parameters were chosen as those giving the best agreement between the experimental $S_{av}(Q)$ and that calculated by analytic Fourier inversion of the model pair correlation function itself. Figure 5 shows the comparison between $S_{av}(Q)$ and the best $S(Q)$ model function. The agreement between the two curves is quite satisfactory with a root-mean-squared error equal to $\simeq 0.05$ on the difference. The model pair correlation function with the parameters fixed by this fitting procedure is shown in Fig. 6 in comparison with the Hartree-Fock result for the homogeneous electron gas.[10] The two curves exhibit a remarkable difference in the region $r < 1$ Å. In particular, the value of the model pair correlation function at $r = 0$, as deduced from the best-fit procedure, turns out to be 0.285. The difference from the corresponding Hartree-Fock value, i.e., 0.5 that follows from the absence of correlations between electrons of antiparallel spin, shows that correlations among opposite-spin electrons cannot be neglected. Therefore a description of electrons in diamond, based on the Pauli principle correlations only, would be inadequate. A much better agreement is found when comparing the $r = 0$ value of the model $\bar{g}(r)$ with the Monte Carlo results for the anisotropic pair correla-

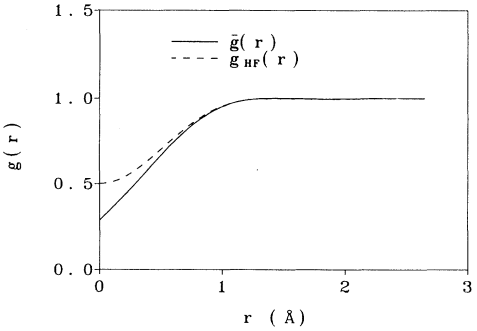

FIG. 6. Model pair correlation function $\bar{g}(r)$ (full line) deduced from the experimental data. The Hartree-Fock result (dashed line) for the homogeneous electron gas calculated at the best-fit value $r_s = 1.15$ is also shown.

tion function.[12,14] In Refs. 12 and 14 the authors found for the pair correlation function the value $\simeq 0.35$ when the first electron is at the bond center and the value $\simeq 0.25$ when the first electron is at the tetrahedral interstitial site. A final observation regards the best-fit value of the parameter r_s, which was also employed in the calculation of the Hartree-Fock pair correlation function (Fig. 6). A value $r_s = 1.15$ was found which is lower than the value 1.32 resulting from the assumption of a homogeneous electron gas for the valence electrons in diamond. Such a discrepancy can be explained by considering the definition of $\bar{g}(\mathbf{r})$ as given in Eq. (8). Since an average over the density is performed, the behavior of the function $\bar{g}(\mathbf{r})$ will be dominated by the high density regions, which correspond to lower values of r_s.

Finally, the information contained in the present scattering experiment can be used to further describe the valence electrons in diamond by calculating the integral,

$$\gamma(r_s) = \frac{1}{2Q_F} \int_0^\infty dQ\,[1 - S(Q)]\ , \tag{10}$$

with Q_F being the Fermi momentum. The function $\gamma(r_s)$, which is a function of r_s alone for the homogeneous electron gas, enters the Hellmann-Feynman theorem[10] and its behavior versus r_s is well known for the electron gas.[5,10] Then $\gamma(r_s)$ calculated through Eq. (10) using the experimental $S_{\text{av}}(Q)$ and assuming $r_s = 1.32$ to represent the valence electrons in diamond as they were a homogeneous gas, can be compared with the value expected for the homogeneous electron gas at the same density.[5] In Fig. 7 the so-calculated value of $\gamma(r_s)$ is superimposed to the curve characteristic of the homogeneous electron system. In such a figure, the experimental value deduced in Be is also reported. Within the quoted error bars, the measured data do not deviate from the theoretical curve. The $\gamma(r_s)$ parameter, whose experimental determination represents an important check to the interacting electron gas theory, is, however, not enough sensible to reveal the anisotropies in the electron distribution as, on the contrary, does the static structure factor.

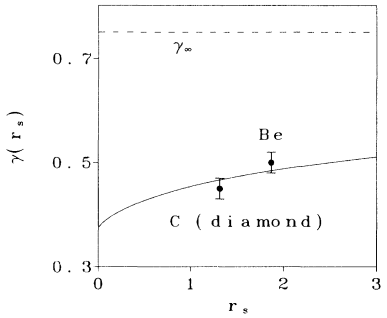

FIG. 7. $\gamma(r_s)$ versus r_s. Full line: theoretical curve for the homogeneous interacting electron gas (Ref. 5). Dots: experimental results for diamond and Be (Ref. 15). γ_∞ (dashed curve) is the theoretical result expected at very high r_s values.

IV. CONCLUSIONS

The analysis of the present experimental data allows us to focus mainly on two aspects of the electron-electron correlations in diamond. A relevant result concerns the exchange and correlation contribution to the cohesive energy. Such a contribution amounts to $\simeq 70\%$ of the total, thus featuring the dynamic correlations as the leading mechanism of cohesion in light elements. An even more pronounced effect was indeed found in the case of Be for which the experimental exchange and correlation contribution to the cohesive energy was about 0.28 Ry, to be compared with the thermodynamic total value 0.25 Ry.

The effect produced by the dynamic correlations is further enhanced by the short-distance behavior of the model pair-correlation function. In particular, an approximate width of the Fermi and Coulomb hole equal to $\simeq 0.6$ Å is found. This finding agrees with the results of the Monte Carlo calculation[12,14] as it also does the value of the pair-correlation function at $r = 0$. Both the experimental and the Monte Carlo results emphasize the inadequacy of accounting for the Fermi hole when describing the valence electrons in diamond.

[1]K. S. Singwi and M. P. Tosi, Solid State Phys. **36**, 177 (1981).
[2]S. Ichimaru, Rev. Mod. Phys. **54**, 1017 (1982).
[3]M. Gell-Mann and K. A. Brueckner, Phys. Rev. **106**, 364 (1957).
[4]E. P. Wigner, Phys. Rev. **46**, 1002 (1934); Trans. Faraday Soc. **34**, 678 (1938).
[5]D. M. Ceperly and B. J. Alder, Phys. Rev. Lett. **45**, 566 (1980).
[6]F. W. King and S. M. Rothstein, Phys. Rev. A **21**, 1373 (1980).
[7]G. D. Mahan, *Many-Particle Physics* (Plenum, New York, 1981).
[8]G. Mazzone and F. Sacchetti, Phys. Rev. B **30**, 1739 (1984).
[9]R. O. Jones and O. Gunnarsson, Rev. Mod. Phys. **61**, 689 (1989).
[10]D. Pines and P. Nozieres, *The Theory of Quantum Liquids* (Benjamin, New York, 1966).
[11]W. Borrmann and P. Fulde, Phys. Rev. B **31**, 7800 (1985).
[12]S. Fahy, X. W. Wang, and S. G. Louie, Phys. Rev. Lett. **65**, 1478 (1990).
[13]X. W. Wang, J. Zhu, S. G. Louie, and S. Fahy, Phys. Rev. Lett. **65**, 2414 (1990).
[14]S. Fahy, X. W. Wang, and S. G. Louie, Phys. Rev. B **42**, 3503 (1990).
[15]G. Mazzone, F. Sacchetti, and V. Contini, Phys. Rev. B **28**, 1772 (1983).
[16]C. B. Walker, Phys. Rev. **103**, 558 (1956).
[17]T. Paakkari and P. Suortti, Phys. Rev. B **9**, 1756 (1974).
[18]F. Sacchetti, Phys. Rev. B **36**, 3147 (1987).
[19]C. Petrillo and F. Sacchetti, Acta Crystallogr. Sec. A **46**, 440

(1990).
[20]R. T. Brown, Phys. Rev. A **5**, 2141 (1972).
[21]R. T. Brown, J. Chem. Phys. **55**, 353 (1971).
[22]A. W. Weiss, Phys. Rev. **162**, 71 (1967).
[23]C. Patel, W. F. Sherman, and G. R. Wilkinson, J. Phys. C **17**, 6063 (1984).
[24]S. W. Lovesey, *Theory of Neutron Scattering from Condensed Matter* (Clarendon, Oxford, 1984), Vol. 1.
[25]A. J. Thakkart and V. H. Smith, J. Phys. **11**, 3803 (1978).
[26]C. Petrillo and F. Sacchetti (unpublished).
[27]M. A. Spackman, Acta Crystallogr. Sec. A **47**, 420 (1991).
[28]A. K. Rajagopal, J. C. Kimball, and M. Banerjee, Phys. Rev. B **18**, 2339 (1978).
[29]V. Contini, G. Mazzone, and F. Sacchetti, Phys. Rev. B **33**, 712 (1986).